Journal of Engineering Physics and Thermophysics, Vol. 81, No. 2, 2008

NUMERICAL ANALYSIS OF THE INFLUENCE OF THE COMPRESSIBILITY OF A VISCOUS GAS ON ITS TURBULENT FLOW AROUND A CYLINDER WITH A CIRCULAR VORTEX CELL

S. A. Isaev, P. A. Baranov, Yu. S. Prigorodov, A. G. Sudakov, and A. E. Usachov

UDC 532.517.4

The influence of the compressibility of a viscous gas flowing around a cylinder with a circular cell on the mechanism of decreasing the drag of the cylinder by suction of air through the withdrawing slot channel in the cell was estimated based on the solution of the stationary Reynolds equations closed using the model of shear-stress transfer, the continuity equations, the energy equation, and the equation of state.

Introduction. In the last decade, considerable attention has been given by researchers of different countries to the study of the possibility to control a flow around bodies with the use of vortex cells built into their surface and a distributed or concentrated blow or suction as well as by rotation of the bodies within the limits of the cells (see, e.g., [1, 2]). One simple test problem on the study of the mechanism of decreasing the drag of bodies by intensification of the flow circulating in the vortex cells built into them is the problem on the laminar and turbulent flows of an incompressible fluid around a cylinder containing a circular cavity with a central body enclosed in it [3–8]. This problem was solved on the assumption that a symmetric flow around a cylinder is provided by a separating plate positioned in the near wake. The progress in investigating this flow was achieved mainly due to the development of computational multiblock technologies for solving the Navier–Stokes and Reynolds equations [1, 9] as well as the improvement of models of turbulence, in particular the appearance of Menter's model of shear-stress transfer [10–13]. Of the results obtained, worthy of mention is first of all the effect of "explosion turbulence" arising at critical rates of rotation or suction in vortex cells due to the jump-like increase in the velocity of the reverse flow to a value comparable to the velocity of the incident flow. In this case, all the integral characteristics experience a discontinuity and the drag decreases due to the expenditure of energy by 36% when the central body is rotated and by 53% when air is sucked from its surface. A rounding of the trailing edge of a vortex cell allows one to additionally decrease the drag of a cylinder by 10%.

The object of the present investigation is two peculiarities of the problem being considered. As already mentioned, a substantial decrease in the drag of a cylinder leads to a marked increase in the intensity of the flow circulating in a cell built into its surface, which allows the conclusion that the compressibility of the medium significantly influences the flow around the cylinder even at moderate Mach numbers. The second peculiarity of this problem is that in it a suction in a vortex cell is considered. As was shown in [9] in the process of calculating the flow around the thick airfoil section of an ÉKIP space craft, the concentrated slot suction from the edges of the cells and the distributed suction from the central bodies are equivalent, i.e., the aerodynamic characteristics of the airfoils having equal flow coefficients are similar independently of the methods of intensification of the flow in their vortex cells. However, the slot suction was realized not entirely correctly because its rate, which was fairly high, was assumed to be constant across the width of the slot in a cell. It is evident that the uniformity of an airfoil is a strong assumption that should be obviated. Therefore, we formulated the problem being considered with the use of a withdrawing channel at the output of which the velocity profile of the sucked-air flow is uniform.

Formulation of the Problem. The interaction of a steady flow of a compressible viscous gas with a transverse cylinder in the absence and in the presence of a circular vortex cell on its surface is calculated on the assump-

St. Petersburg State University of Civil Aviation, 38 Pilotov Str., St. Petersburg, 196210, Russia; email: isaev @SI3612spb.edu. Translated from Inzhenerno-Fizicheskii Zhurnal, Vol. 81, No. 2, pp. 330–337, March–April, 2008. Original article submitted October 3, 2006.

1062-0125/08/8102-0351

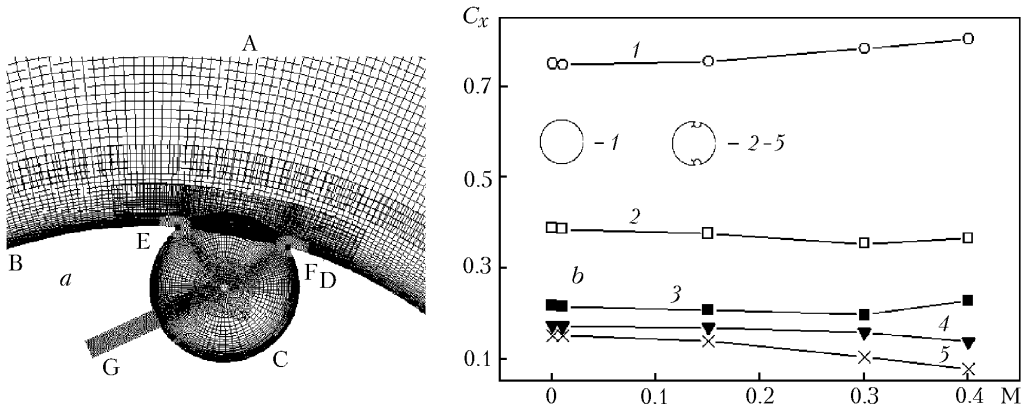

Fig. 1. Multiblock computational grids (A–G) near the vortex cell with a withdrawing channel on the surface of a cylinder (a) and dependences of the total drag (curves 1, 2), drag (3), and the additional drag caused by the expenditure of energy (4), the drag of the cylinder in the absence (1) and in the presence (2–4) of a vortex cell, and the mass-flow coefficient in the withdrawing channel (5) on the Mach number (b).

tion that the gas flow is symmetric and its adiabatic coefficient is equal to 1.4 (air). A stationary plane motion of the medium in the upper semiplane of the cylindrical computational region with a symmetry plane is considered. The center of the cylinder is coincident with the origin of the Cartesian coordinate system x, y. The outer boundary of the computational region is at a large distance (35 cylinder diameters) from the center of the cylinder. The parameters of the flow at the input boundary are fixed. The density and velocity of the flow and the diameter of the cylinder are taken as the dimensionless scales. The soft boundary conditions (the conditions of continuation of solution) are set at the output boundary and the symmetry conditions are set in the symmetry plane. The parameters of turbulence at the input to the computational region are selected in the same manner as in the case of solution of the problem on a flow of an incompressible viscous fluid [1, 9]: it is assumed that the degree of turbulence of the external flow is at a level characteristic of a wind tunnel (Tu = 1.5%) and the scale of turbulence is equal to the diameter of the cylinder. The adhesion condition is set at the walls. The Reynolds number Re_∞ is taken to be equal to $1.5 \cdot 10^4$, which corresponds to the experimental value of Re determined in the experiments carried out in a wind tunnel by Roshko [14]. The Mach number M_∞ is varied from 0 to 0.4.

The vortex cell built into the surface of the cylinder being considered represents a circular cavity of radius 0.08 (Fig. 1a). This cavity is positioned such that the separation point travels from the windward of the circular cylinder to its lee side; the position of the cavity is selected based on the experience in solving analogous problems [3–8]. The coordinates of the center of the cell are $x = 0.0772$, $y = 0.4339$. The radius of rounding of the cavity edges is taken to be equal to $1.012 \cdot 10^{-3}$, i.e., it is assumed that these edges are sharp. A withdrawing slot channel of width 0.02 and length 0.08 is positioned along the normal to the surface of the cell at an angle of 145° to the outer normal to the cylinder, passing through the center of the cell. It is assumed that the volumetric rate of flow through the channel is equal to 0.015.

Computational Grids. Structured multiblock grids are introduced for calculating the air flow in a multiply connected, many-scaled zone positioned near the cylinder with a cell (Fig. 1a). The multistage grids denoted by A and B are used for correct definition of the near-wall boundary layer and the separation region in the wake downstream of the cylinder. The grid A consists of two stages representing concentric grid layers, in which nodes are identically distributed along the radius. In the layer of thickness 7, positioned near the cylinder, a fairly coarse grid, containing 220 cells, is constructed for representation of the large-scale vortex zone. In the far layer (60 cells) of length of up to 35 cylinder diameters, the grid pitch in the radial direction increases monotonically. The stage of cells B of small thickness 0.07, adjacent to the surface of the cylinder, is used for definition of the developing boundary layer. In it, 40 cells are arranged in the radial direction and the near-wall pitch is equal to 10^{-4}. The cells in this grid are distributed nonuniformly over the circumference of the cylinder with a bunching of nodes to the back critical point, and the grid

pitch is equal to $2 \cdot 10^{-3}$. At the front critical point, the grid pitch is assumed to be equal to 10^{-2}. The total number of cells positioned along the circumference of the cylinder is equal to 320 without of a vortex cell and 290 for the cylinder with a vortex cell.

The concentric grid C (with a hole of diameter 0.0096 at the center) defines the distribution of computational cells in the circular cavity. In this grid, as in the above-described grids, nodes are arranged in the radial direction with a bunching to the edges of the cavity. The near-wall pitch is equal to 10^{-4}. Along the radius, 40 cells are positioned. In the circumferential direction, nodes are arranged very nonuniformly. The grid is bunched predominantly in the neighborhood of the sharp edges and in the region of the slot hole. In the region of the "cavity window," 40 cells are positioned, and 80 cells are arranged along the contour of the cavity.

The central zone of the cavity, coincident with the hole of the concentric grid C, is covered by a square, rectangular grid ("patch") of size 0.05×0.05, containing 16×16 cells distributed uniformly. This grid is introduced for prevention of the near-axis troubles characteristic of the calculations carried out with the use of cylindrical grids [1].

The origin of the withdrawing slot channel is covered by a rectangular grid G with cells (15) distributed uniformly across the channel and nonuniformly along it; in this case, the grid pitch increases from 10^{-4} to $5 \cdot 10^{-4}$ with increase in the distance from the hole.

To increase the accuracy of definition of the vortex flow in the neighborhood of the cavity window, we introduced a curvilinear three-section grid D containing 90×30 cells, adjacent to the window. The left and right fragments of this grid represent cylindrical grids joined to the surface of the cylinder, and its central part positioned immediately above the window of the cavity represents a Scalence grid with a lower and upper rectilinear generating lines. The thickness of the grid layer is 0.035.

Note that it is necessary to correctly define the features of the flow in the neighborhood of the rounded sharp edges, where the special fine grids E and F of size 38×15 cells are arranged.

Features of the Computational Algorithm. The derivation of multiblock computational technologies realized in the VP2/3 package used for solving problems on separation incompressible-fluid flows around bodies with vortex cells was described in detail in [1]. The approach to the solution of the Reynolds equations is based on the known method of splitting by physical processes within the framework of the SIMPLEC procedure of pressure correction [15]. The equation for the pressure correction is written instead of the continuity equation, which is entirely warranted for incompressible-fluid flows. However, this method of solving the problem being considered is not unique. For example, the method of artificial compressibility [15] is sometimes used for this purpose; it allows one to construct a marching algorithm for solving the system of equations for an unknown vector (velocity components, pressure). This method correlates well with the methods of solving the equations for a compressible viscous gas that differ substantially from the methods of pressure correction and have a limited application at low Mach numbers.

The derivation of the generalized procedure of pressure correction, which would be equally applied to incompressible-fluid and compressible-gas flows, was a pressing problem in the 1980s. This problem was solved in a number of works (see, e.g., [16, 17]). A separate problem is the calculation of flows with compression shocks that can be fairly strong at Mach numbers larger than unity.

The generalized algorithms for pressure correction, developed earlier [15–17], were realized principally with the use of multiblock grids with no account for the modern semiempirical models of turbulence. The problem on construction of the generalized multiblock algorithm for pressure correction was solved to advantage in the process of calculating airfoils with holes [18]. The starting works are monographs [1, 9] and articles by Menter with co-authors and Hellsten [10–13, 19], devoted to the methodical aspects on simulation of turbulence, in particular to the model of shear-stress transfer used in the present investigation. An important feature of the algorithm developed for calculating compressible turbulent flows, including flows with compression shocks, is its applicability to simulation of incompressible flows. The methodical calculations of nonviscous flows with compression shocks (see, e.g., [18]) have shown that, from the standpoint of computational-process stability, it is appropriate to approximate the convective members of the Reynolds equations by the Leonard scheme and the convective members of the other equations by the Van-Lir scheme.

Analysis of Calculation Data. Some of the results obtained are presented in Figs. 1–5 and in Tables 1–3.

As follows from Fig. 1b, the drag of a circular cylinder increases monotonically with increase in the Mach number of the incident flow in the same way as the drag of a cylinder with a bulging coaxial disk increases in the case of an axisymmetric flow around it [20]. As is seen from Table 1, C_{xc} increases due to the increase in the pres-

TABLE 1. Influence of the Compressibility on the Integral Characteristics of the Circular Cylinder in the Absence and in the Presence of a Vortex Cell

Mach number	Cylinder		Cylinder with a vortex cell	
	C_{xp}	C_{xf}	C_{xp}	C_{xf}
0 [14]	0.72	—	—	—
0 [21]	0.732	0.011	—	—
0 [1]	0.729	0.019	—	—
0	0.734	0.017	0.202	0.014
0.01	0.731	0.017	0.200	0.014
0.15	0.739	0.017	0.193	0.014
0.3	0.767	0.017	0.184	0.011
0.4	0.789	0.017	0.217	0.011

TABLE 2. Influence of the Mach Number on the Decrease in the Relative Drag of the Cylinder with a Vortex Cell

Mach number	0	0.01	0.15	0.3	0.4
$C_{xc}/C_{xc.v}$	1.94	1.94	2.02	2.22	2.21

TABLE 3. Influence of the Compressibility on the Extremum, Local Characteristics of the Flow around the Cylinder in the Absence and in the Presence of a Vortex Cell

Mach number	Cylinder				Cylinder with a vortex cell			
	u_m	ρ_m	k_m	$\mu_{t,m}$	u_m	ρ_m	k_m	$\mu_{t,m}$
0	–0.244	1	0.0913	0.0276	–0.199	1	0.1098	0.00873
0.01	–0.236	1	0.0889	0.0272	–0.199	1	0.1082	0.00911
0.15	–0.238	0.985	0.0897	0.0270	–0.192	0.896	0.0962	0.00924
0.3	–0.242	0.939	0.0907	0.0264	–0.167	0.657	0.0761	0.00858
0.4	–0.245	0.893	0.0916	0.0259	–0.163	0.487	0.0773	0.01030

sure drag C_{xp}, while the friction drag C_{xf} remains constant. It is interesting to note that the results of calculations of C_{xp} at $M_\infty = 0$, i.e., for an incompressible fluid, are in good agreement with the analogous results of the calculations carried out earlier [1, 21] and the corresponding experimental data [14].

The arrangement of a circular cavity with a withdrawing channel on the surface of the cylinder being considered and organization of a suction with a constant volumetric rate of flow (Fig. 1a) makes it possible to decrease the calculated drag of the cylinder by almost two times (curve 3 in Fig. 1b). When the Mach number increases, C_x changes in the same manner as the drag of the circular cylinder with no a vortex cell, i.e., it increases monotonically with increase in the pressure drag C_{xp} (Table 1). In this case, the friction drag of the cylinder with a cavity remains unchanged and lower by approximately 20% than the friction drag of the usual cylinder.

The additional drag $C_{x\text{add}}$ (curve 4) caused by the expenditure of energy for the suction, determined by the method proposed in [1], decreases monotonically with increase in the Mach number M_∞ predominantly due to the decrease in the coefficient of mass flow through the withdrawing channel c_q (curve 5). As a result, the total drag of the cylinder with a vortex cell $C_{xc.v}$ somewhat decreases at M_∞ changing within the range 0–0.4 being considered (curve 2). Hence, the ratio $C_{xc}/C_{xc.v}$ (see Table 2) increases monotonically with increase in the Mach number and reaches a maximum at $M_\infty = 0.3$.

The distributions of the longitudinal velocity $u(x)$ and the density $\rho(x)$ in the symmetry plane in the wake downstream of the cylinder in the absence and in the presence of a vortex cell on its surface are very different in the case where M_∞ increases (Fig. 2). In the range of change in M_∞ from 0 to 0.3, the profiles of $u(x)$ are practically identical (Fig. 2a), while $\rho(x)$ depends substantially on M_∞. As is seen from Fig. 2b, the largest rarefaction is attained in the circulation flow in the near wake downstream of the cylinder, and the level of this rarefaction is markedly larger for the circular cylinder than for the cylinder with a vortex cell.

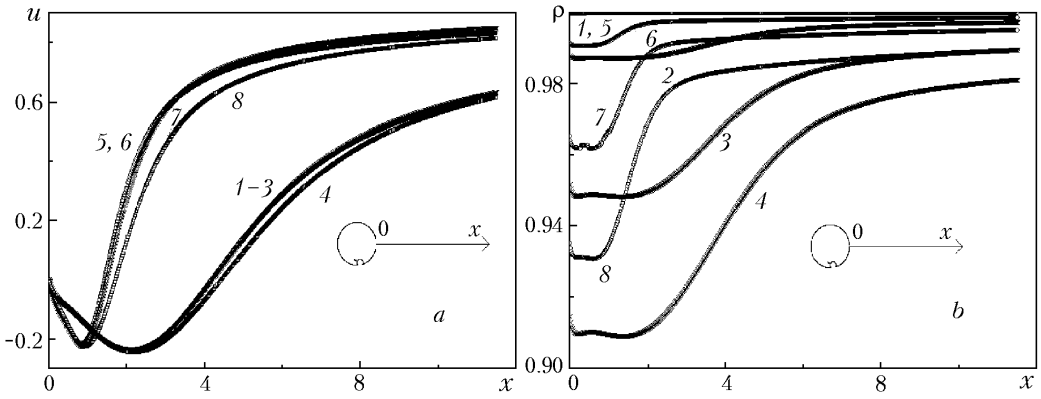

Fig. 2. Distribution of the longitudinal velocity component u (a) and the air density ρ (b) along the symmetry axis x beginning at the back critical point of the cylinder in the absence (1–4) and presence (5–8) of a vortex cell for different Mach numbers: M_∞ = 0.01 (1, 5), 0.15 (2, 6), 0.3 (3, 7), and 0.4 (4, 8).

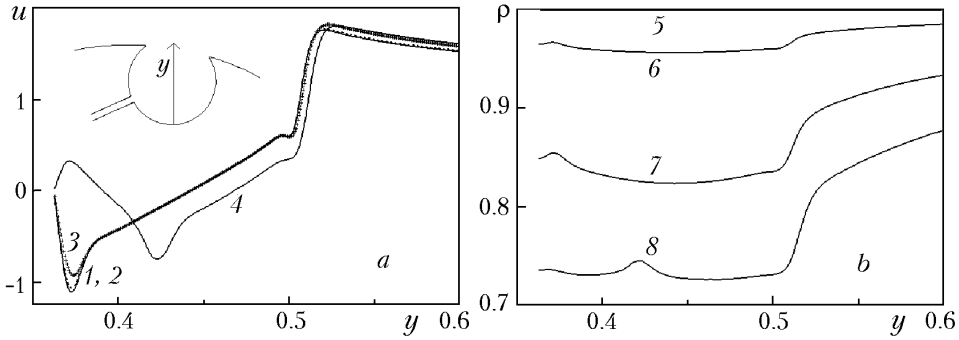

Fig. 3. Profiles of the longitudinal component u (a) and the air density ρ (b) at the middle cross section of the circular cavity along the y axis in the absence (1–4) and presence (5–8) of a vortex cell on the cylinder for different Mach numbers: M_∞ = 0.01 (1, 5), 0.15 (2, 6), 0.3 (3, 7), and 0.4 (4, 8).

As is seen from Table 3, the extremum parameters of the flows around the usual smooth cylinder and the cylinder with a cavity and their characteristics of turbulence change in the opposite manners depending on the compressibility. True, the quantitative changes are small. With increase in M_∞, the maximum velocity of the reverse flow in the wake downstream of the smooth cylinder increases and this velocity downstream of the cylinder with a cell decreases monotonically. The maximum energies of turbulence k_m behave analogously, while the maximum eddy-viscosity coefficients $\mu_{t,m}$ change in the opposite manner.

As follows from Fig. 3a, an increase in the number M_∞ leads to a decrease in the maximum velocity of the flow circulating in the vortex cell; this velocity decreases to approximately 85% of the external-flow velocity with increase in M_∞ from 0 to 0.3. The longitudinal velocity u further decreases at M_∞ = 0.4. As was shown earlier in investigating the change in the drag, the reason for the indicated effect is first of all the large change in the mass-flow coefficients (curve 5 in Fig. 1b). This decrease is mainly due to the rarefaction in the region of the vortex cell (Fig. 3b), which is much larger than the rarefaction in the near wake downstream of the cylinder and increases with increase in M_∞ (Fig. 2b). It is notable that the dependence $u(y)$ in the central part of the circular cavity is near-linear and remains unchanged in the range of change in M_∞ 0–0.3, i.e., under the conditions where one large-scale vortex exists in the vortex cell. The core of a constant-vorticity vortex is practically nonviscous, i.e., the Batchelor hypothesis on the existence of a nonviscous vortex surrounded by a boundary layer is fulfilled in the vortex cell [1].

As follows from Fig. 4, a vortex cell built into the surface of a cylinder substantially restructures the flow in the near wake. The separation point on the surface of the cylinder is shifted downstream of the circular cavity, and

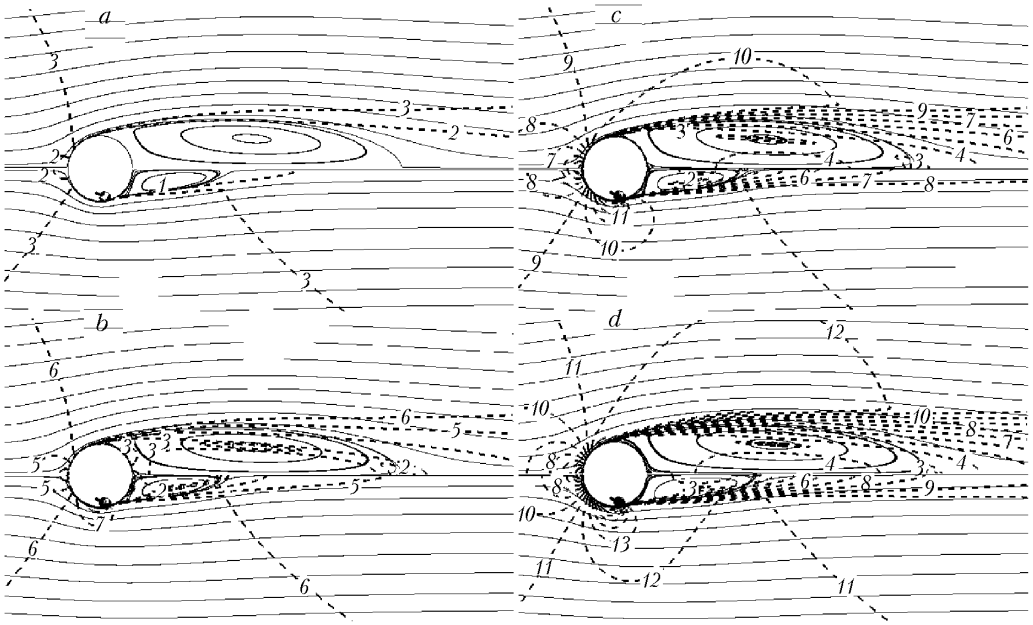

Fig. 4. Comparative analysis of the patterns of flow around a cylinder (upper semiplanes) and a cylinder with a vortex cell (lower semiplanes): M_∞ = 0.01 (a), 0.15 (b), 0.3 (c), and 0.4 (d); M = 0.0001 (1), 0.005 (2), 0.01 (3), 0.05 (4), 0.1 (5), 0.15 (6), 0.2 (7), 0.25 (8), 0.3 (9). 0.35 (10), 0.4 (11), 0.45 (12), and 0.5 (13).

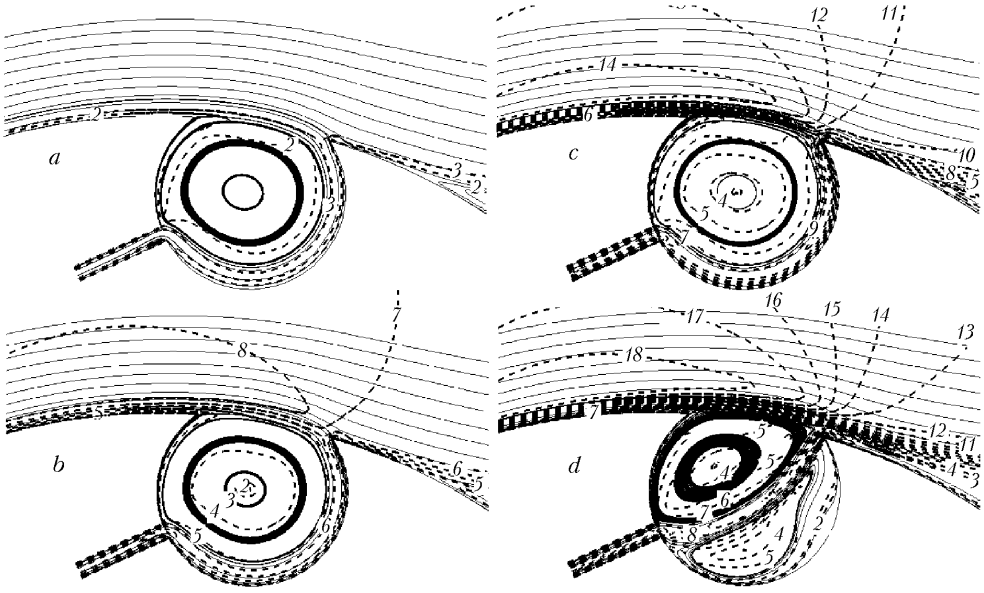

Fig. 5. The pattern of flow in the neighborhood of a vortex cell on the cylinder: M_∞ = 0.01 (a), 0.15 (b), 0.3 (c), and 0.4 (d); the isomaches are identical to those in Fig. 4; M = 0.55 (14), 0.6 (15), 0.65 (16), 0.7 (17), and 0.75 (18).

the length of the circulation zone is three times smaller as compared to the cylinder with no a cavity. An increase in the number M_∞ has no a significant influence on the pattern of the separation flow around the body — analysis of Fig. 2a shows that the longitudinal velocity of the flow in the wake downstream of the cylinder changes insignificantly. However, the field of local Mach numbers and the density distributions in the wake change significantly (Fig. 2b), and these changes are much larger for the cylinder with a vortex cell than for the usual cylinder. For example, at

M_∞ = 0.4, in the neighborhood of the side surface of the cylinder with no a cavity the local Mach number increases by only 0.1 and reaches 0.5. At the same time, for the cylinder with a vortex cell the maximum local Mach numbers exceed 0.75, i.e., they are close to the transonic Mach numbers.

The suction of air into the withdrawing channel in a circular cavity is similar in many respects to the boundary-layer drain [1] (see Fig. 5). In any event, in the flow patterns presented, the near-wall layer in the neighborhood of the vortex cell is clearly defined; this layer flows into the cell and then is transformed into the slot channel. The high-intensity large-scale vortex, caught by the cell, is kept against the windward part of the cavity surface. The formation of a local separation at the input to the withdrawing channel points to the fact that the velocity profile at this site is significantly nonuniform. Thus, the organization of a concrete concentrated suction is warranted, i.e., the process of control of the flow around bodies by the method being considered should be analyzed with consideration for the method of intensification of the flow circulating in the vortex cell.

As was mentioned above, in the range of change in M_∞ from 0 to 0.3, the pattern of the vortex flow remains practically unchanged, even though the influence of the compressibility on the field of local Mach numbers is evident. At M_∞ = 0.4, in the cavity there arises a large-scale secondary vortex, and the separation point on the surface of the cylinder shifts to the neighborhood of its trailing edge and a portion of air from the near wake is entraped by the vortex cell. As follows from Fig. 3a, the cores of the primary and secondary vortices in the cell have a constant vorticity and are practically nonviscous. However, the intensity of these vortices is much lower than the intensity of the vortex at smaller values of M_∞.

Thus, in the case where the volumetric rate of flow of the sucked air remains unchanged, the decrease in the drag of a cylinder, provided by a vortex cell built into its surface, is limited by the Mach number M_∞ = 0.4.

This work was carried out with financial support from the Russian Foundation for Basic Research (projects No. 06-08-81002 and No. 05-02-00162) and the European-Union Framework-6 program (VortexCell2050 project).

NOTATION

a, velocity of sound, in fractions of U; C_x, C_{xp}, C_{xf}, drag, profile-drag, friction-drag related to the kinetic head, in fractions of $\rho U^2/2$; c_q, mass flow of the air sucked through the slot channel; D, diameter of the cylinder, m; M, Mach number ($M = q/a$); k, energy of turbulence, in fractions of U^2; q, modulus of the local velocity of a flow, in fractions of U; Re, Reynolds number ($Re = \rho UD/\mu$); Tu, degree of turbulence, in fractions of U; x, y, horizontal and vertical coordinates; in fractions of D; U, velocity of a uniform flow, m/sec; u, longitudinal velocity component, in fractions of U; μ, coefficient of dynamic viscosity, kg/(m·sec); ρ, density, kg/m^3. Subscripts: add, additional drag caused by the expedience of energy; c, c.v, characteristics for the smooth cylinder and the cylinder with a vortex cell; m, maximum values; t, characteristics of turbulence; ∞, value in the incident flow.

REFERENCES

1. A. V. Ermishin and S. A. Isaev (Eds.), *Control of Flow Past Bodies with Vortex Cells as Applied to Aircraft of Integrated Layout* (*Numerical and Physical Modeling*) [in Russian], MGU, Moscow (2003).
2. C. Wang and M. Sun, Separation control on a thick airfoil with multiple slots blowing at small speeds, *Acta Mechanica*, **143**, 215–227 (2000).
3. P. A. Baranov, S. A. Isaev, Yu. S. Prigorodov, and A. G. Sudakov, Numerical simulation of a laminar flow past a cylinder with passive and active vortex cells within the framework of the concept of decomposition of a computational domain and with the use of multistage grids, *Pis'ma Zh. Tekh. Fiz.*, **24**, Issue 8, 33–41 (1998).
4. P. A. Baranov, S. A. Isaev, Yu. S. Prigorodov, and A. G. Sudakov, Numerical simulation of the effect of the decrease in the drag of a cylinder with vortex cells in the presence of the system for control of the turbulent boundary layer, *Pis'ma Zh. Tekh. Fiz.*, **24**, Issue 17, 16–23 (1998).
5. P. A. Baranov, S. A. Isaev, and A. G. Sudakov, Numerical simulation of the influence of the generated vorticity on the von Kármán vortex street down stream of a circular cylinder, *Izv. Ross. Akad. Nauk*, *Mekh. Zhidk. Gaza*, No. 2, 68–74 (2000).

6. S. A. Isaev, Yu. S. Prigorodov, and A. G. Sudakov, Numerical analysis of the efficiency of vortex cells in the case of laminar and turbulent flows around a circular cylinder with rotating bodies built into it, *Izv. Ross. Akad. Nauk*, *Mekh. Zhidk. Gaza*, No. 4, 88–96 (2000).
7. S. A. Isaev, Yu. S. Prigorodov, and A. G. Sudakov, Analysis of the efficiency of control of a flow around bodies with the use of vortex cells with allowance for the expenditure of energy, *Inzh.-Fiz. Zh.*, **75**, No. 3, 47–50 (2002).
8. P. A. Baranov, S. A. Isaev, Yu. S. Prigorodov, and A. G. Sudakov, Numerical analysis of the influence of the shape of the vortex cells built into a circular cylinder on a steady turbulent flow around it, *Inzh.-Fiz. Zh.*, **76**, No. 6, 38–44 (2003).
9. Yu. A. Bystrov, S. A. Isaev, N. A. Kudryavtsev, and A. I. Leontiev, *Numerical Simulation of the Vortical Intensification of the Heat Transfer in Tube Banks* [in Russian], Sudostroenie, St. Petersburg (2005).
10. F. R. Menter, Zonal two-equation k–ω turbulence models for aerodynamic flows, *AIAA Paper*, No. 93–2906 (1993).
11. F. R. Menter, M. Kuntz, and R. Langtry, Ten years of industrial experience with the SST turbulence model, in: K. Hanjalic, Y. Nogano, and M. Tummers (Eds.), *Turbulence*, *Heat and Mass Transfer 4*, Begell House, Inc., New York (2003).
12. F. Menter, J. C. Ferreira, T. Esch, and B. Konno, Turbulence model with improved wall treatment for heat transfer predictions in gas turbines, *Proc. Int. Gas Turbine Congress*, November 2–7, 2003, Tokyo (2003).
13. T. Esch and F. R. Menter, Heat transfer predictions based on two-equation turbulence models with advanced wall treatment, in: K. Hanjalic, Y. Nogano, and M. Tummers (Eds.), *Turbulence*, *Heat and Mass Transfer 4*, Begell House, Inc., New York (2003).
14. A. Roshko, Experiments on the flow past a circular cylinder at very high Reynolds number, *J. Fluid Mech.*, **10**, 345–356 (1961).
15. J. H. Ferziger and M. Peric, *Computational Methods for Fluid Dynamics*, Heidelberg, Berlin (1999).
16. K. C. Karki and S. V. Patankar, Pressure-based calculation procedure for viscous flows at all speeds in arbitrary configuration, *AIAA J.*, **27**, 1167–1174 (1989).
17. W. Shyy, M. H. Chen, and C.-S. Sun, Pressure-based multigrid algorithm for all speeds, *AIAA J.*, **30**, No. 11, 2660–2669 (1992).
18. S. A. Isaev, A. I. Leontiev, A. G. Sudakov, and P. A. Baranov, Numerical simulation of supersonic flow around a dimpled surface, *Minsk Int. Colloq. on Physics of Shock Waves*, *Combustion*, *Detonation and Non-Equilibrium Processes*, MIC2005, Minsk (2005), pp. 48–49.
19. A. Hellsten, Some improvements in Menter's k–ω turbulence model, AIAA-98-2554 (1998).
20. V. K. Bobyshev and S. A. Isaev, Numerical investigation of the effect of compressibility on the mechanism of decreasing the drag of a cylinder with organized stall regions in a turbulent flow, *Inzh.-Fiz. Zh.*, **71**, No. 4, 606–612 (1998).
21. I. A. Belov and N. A. Kudryavtsev, *Heat Transfer and Resistance of a Tube Bank* [in Russian], Énergoatomizdat, Leningrad (1997).

Fig. 1. Multiblock computational grids (A–G) near the vortex cell with a withdrawing channel on the surface of a cylinder and dependences of the total drag (curves 1, 2), drag (3), and the additional drag caused by the expenditure of energy (4), the drag of the cylinder in the absence (1) and in the presence of a vortex cell, and the mass-flow coefficient in the withdrawing channel (5) on the Mach number.